Aza-BODIPY Platform: Toward an Efficient Water-Soluble Bimodal Imaging Probe for MRI and Near-Infrared Fluorescence

Océane Florès, Jacques Pliquett, Laura Abad Galan, Robin Lescure, Franck Denat, Olivier Maury, Agnès Pallier, Pierre-Simon Bellaye, Bertrand Collin, S. Même, et al.

Aza-BODIPY Platform: Towards an Efficient Water-Soluble Bimodal Imaging Probe for MRI and Near-Infrared Fluorescence

Océane Florès[a], Jacques Pliquett[a], Laura Abad-Galan[b], Robin Lescure[a], Franck Denat[a], Olivier Maury[b], Agnès Pallier[c], Pierre-Simon Bellaye[d], Bertrand Collin[a-d], Sandra Même[c], Célia S. Bonnet[c]*, Ewen Bodio[a]*, Christine Goze[a]*.

[a] CNRS, Université Bourgogne Franche-Comté, ICMUB UMR6302 – CNRS, F-21000 Dijon, France.
[b] Univ Lyon, Ecole Normale Supérieure de Lyon, CNRS, Université Claude Bernard Lyon 1, Laboratoire de Chimie, UMR 5182, F-69342 Lyon, France.
[c] Centre de Biophysique Moléculaire, CNRS, Université d'Orléans, Rue Charles Sadron, 45071 Orléans Cedex 2, France.
[d] Centre Georges François Leclerc, Service de médecine nucléaire (plateforme d'imagerie et de radiothérapie précliniques), 1 rue Professeur Marion, BP77980, 21079 Dijon Cedex

Abstract

In this study, an original aza-BODIPY system comprising two Gd^{3+} complexes has been designed and synthesized for magnetic resonance imaging/optical imaging application, by functionalization of the boron center. This strategy enabled to obtain a positively-charged bimodal probe, which displays an increased water-solubility, optimized photophysical properties in the near-infrared region, and very promising relaxometric properties. The absorption and emission wavelengths are 705 and 741 nm respectively, with a quantum yield of around 10 % in aqueous media. Moreover, the system does not produce singlet oxygen upon excitation, which would be toxic for tissues. The relaxivity obtained is high at intermediate fields (16.1 $mM^{-1}.s^{-1}$ at 20 MHz and 310 K) and competes with that of bigger or more rigid systems. A full relaxometric and ^{17}O NMR study and fitting of the data using the Lipari-Szabo approach showed that this high relaxivity can be explained by the size of the system and the presence of some small aggregates. These optimized photophysical and relaxometric properties highlight the potential use of such systems for future bimodal imaging studies.

Introduction

Imaging and especially molecular imaging has gained an increasing interest during these last years. Indeed, the insights in this field facilitate an earlier and more reliable diagnostic, enable the monitoring of the efficiency of a therapy, and even assist the surgeon during operations.[1–6] Therefore, molecular imaging can benefit to a large number of pathologies. Moreover, this imaging approach also permits the discovery of novel biological targets or biomarkers and help to understand mechanisms of different diseases. Each molecular imaging technique has its own advantages and drawbacks and synergy is expected by association of two complementary modalities in a single molecular probe.[7] This is particularly true when combining the two non-ionizing techniques: Magnetic Resonance Imaging (MRI) with Optical Imaging (OI). Indeed, MRI has an excellent spatial resolution and offers 3D anatomical and also functional information, which is ideal for *in vivo* imaging, but it suffers from low sensitivity. On the other hand, OI exhibits high sensitivity and high microscopic resolution (<10 nm in the case of super resolved fluorescent microscopy), but suffers from poor tissue penetration.[8] Another advantage of OI is that it enables real time imaging. Moreover, more recently, despite its limited penetration depth, it has gained an increasing interest *in the clinic* for intra-operative fluorescence assisted surgery, where the use of fluorescence imaging

particularly helps the surgeon to better delineate tumor margins, identify the lymph nodes invaded by cancer cells…[9]

In order to perform bimodal MRI/OI, there is an increasing interest in the conception of new efficient multimodal probes. Indeed, combination of these two imaging modalities into a single molecule assures the identical biodistribution compared to the combination of two separate imaging agents, and thus enables to perform a much more accurate diagnosis. The design of such bimodal probes is a real challenge, mainly because of the difference of sensitivity between MRI and OI. Therefore, the majority of the reported MRI/OI agents are based on functionalized polymers or nanoparticles. However small molecular bimodal agents were also reported and proved to be very effective. These agents combine fluorine atoms for ^{19}F MRI or one, two, or more complexes, which are active in MRI, such as Mn^{2+} or Gd^{3+} complexes, and one fluorophore, which can be a dipyridophenazine, fluorescein, cyanine, rhodamine, quinoline, BODIPY...[10–18]

For *in vivo* optical imaging applications, the fluorophores need to absorb and emit in the spectral range, where biological tissues are more transparent and less scattering. This region, often called biological, transparency or theranostic window, corresponds to near infrared (NIR, as example NIR I corresponds to 650-900 nm).[19–21] Development of NIR fluorophores is a hot topic because, despite the diversity of reported fluorophores, it seems that none of them is ideal for *in vivo* applications, and that most of them lack of chemical and photochemical stability, are poorly water soluble, low emissive, difficult to functionalize and their synthesis is time-consuming.[22–25] Very recently, the aza-BODIPY family attracted considerable attention because it may be one of the best candidates to tackle all these issues. These very stable BODIPY derivatives display a lower brightness than well-known NIR cyanines such as ICG and IRDye® 800CW (Figure 1), but can be rapidly synthesized in large scale and are easily functionalized.[26]

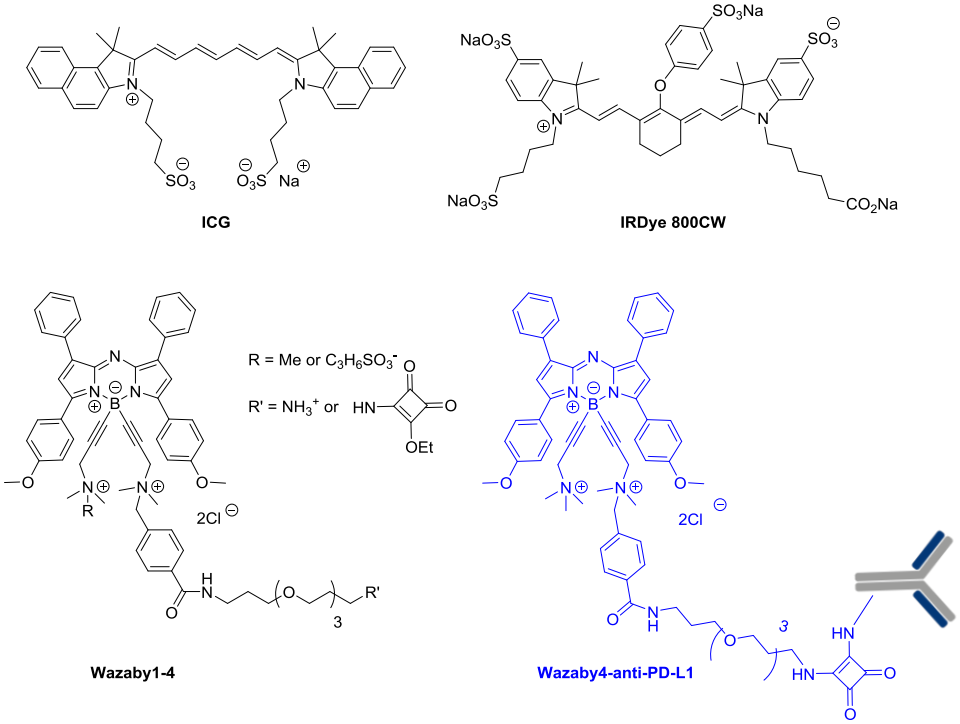

Figure 1: structure of some optical imaging clinically used contrast agents and of Wazaby (water-soluble aza-BODIPY), we reported previously[27]

However, despite their potential, there are only very scarce reports of bimodal MRI/OI probes including (aza)-BODIPY. They have been used in combination with several fluorine atoms for ^{19}F MRI,[17] or with two GdDTPA complexes,[28] or GdDOTA complexes in a monomolecular system[13] or in a polyrotaxane[29]. The sensitivity of ^{19}F MRI remains lower than that of ^{1}H MRI. GdDTPA complexes are

not the best candidates for *in vivo* use (*vide infra*) and the relaxivity of the BODIPY-GdDOTA system (*vide infra*) can certainly be optimized. This leaves room for improvement of such systems. It should also be noted that a bisGdDTPA-aza-BODIPY system was recently reported by Kim, Long and coll. to track *in vivo* phagocytic immune cells by MRI/OI bimodal imaging, highlighting the potential of such systems.[28]

Despite their interesting properties, the limited use of BODIPY in bimodal imaging can certainly be explained by their poor water solubility, which is problematic for their use *in vivo*, and particularly for MRI.[30–32] Several groups tethered water-solubilizing groups to the aza-BODIPY core, but even if sometimes it enabled *in vitro* and *in vivo* investigations, the resulting probes were still subject to significant aggregation phenomena (requiring the addition of surfactant).[30,33,34] Very recently, some of us succeeded in designing fully water-soluble aza-BODIPY derivatives, called Wazaby (for water-soluble aza-BODIPY), thanks to the introduction of ammonium groups *via* boron functionalization (functionalizing boron induced aza-BODIPY faces hindrance, which prevented aggregation) (Figure 1).[27] These probes were bioconjugated onto antibodies, were very stable in physiological media, and presented better *in vivo* optical properties than the Cy5, used as a control.

Building on this success, we decided to further investigate the potential of these Wazaby dyes and to conceive MRI/OI MOnomolecular Multimodal Imaging Probes (MOMIP). For this aim, we decided to attach two gadolinium complexes onto the boron-functionalized arms of the Wazaby scaffold, thanks to the strategy developed previously (Figure 2). Concerning the aza-BODIPY core, we chose an aza-BODIPY bearing methoxy groups on the aromatic rings at the "south" of the molecule (also called proximal phenyl groups in aza-BODIPY chemistry) in order to shift the maximal absorption wavelength around 690-700 nm. To maximize this effect (maximal absorption wavelength >700 nm) by creating a greater "push-pull" effect, bromine atoms were introduced on the aromatic rings at the "north" of the molecule (distal phenyl groups). It has to be noted that this functional group would enable further functionalization of the molecule in the future (extension of conjugation or introduction of a bioconjugatable handle if vectorization is needed).[35]

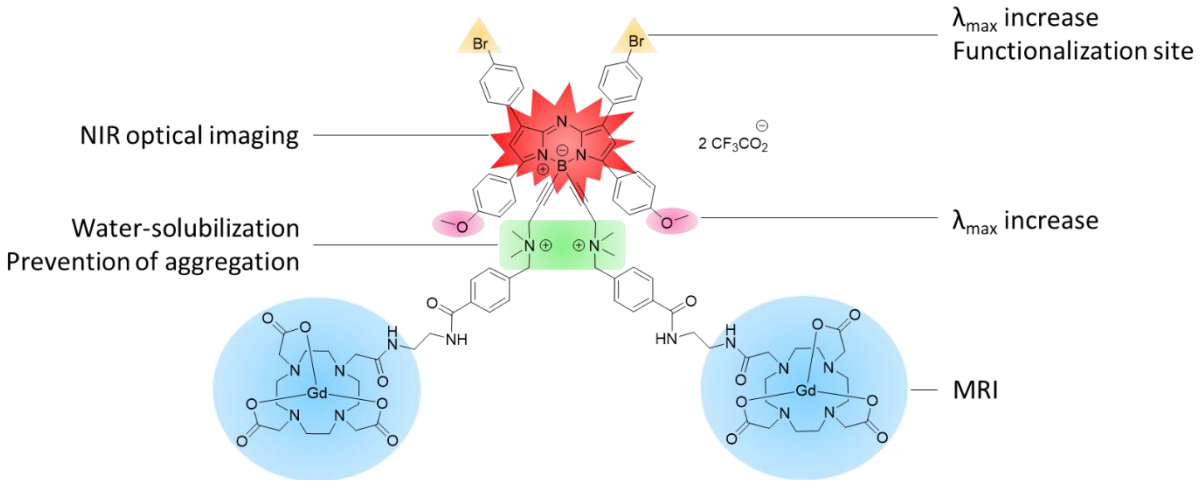

Figure 2 : Targeted bimodal probe and justification of the chosen functionalization

In MRI, DOTAREM® is one of the most clinically used contrast agents due to its high thermodynamic stability and kinetic inertness, which is essential for the safe use of the probe.[36] Indeed, free gadolinium ions are highly toxic, and recently, complexes with lower kinetic inertness have been shown to increase the risk of nephrogenic systemic fibrosis (NSF), especially for patients having renal failure.[37] As macrocyclic chelates are known to be more stable than linear ones, a DOTA derivative (DOTA monoamide or DOTAMA) was used for Gd^{3+} complexation.

Results and Discussion

Synthesis

Aza-BODIPY **2** was synthesized at the gram scale according to the method we previously reported,[27] starting by the synthesis of the aza-BODIPY **1**,[38] followed by the substitution of the fluorine atoms on the boron center using the Grignard reagent of *N*,*N*-dimethylpropargylamine. The resulting intermediate platform was then alkylated by an excess of 4-(bromomethyl)benzoic acid in presence of $NaHCO_3$ (Scheme 1) to give **Wazaby5**. Special attention was paid to the base employed as proton scavenger. A stronger base led to the formation of small amount of ester side product – alkylation of the carboxylate –, leading to a tricky purification.

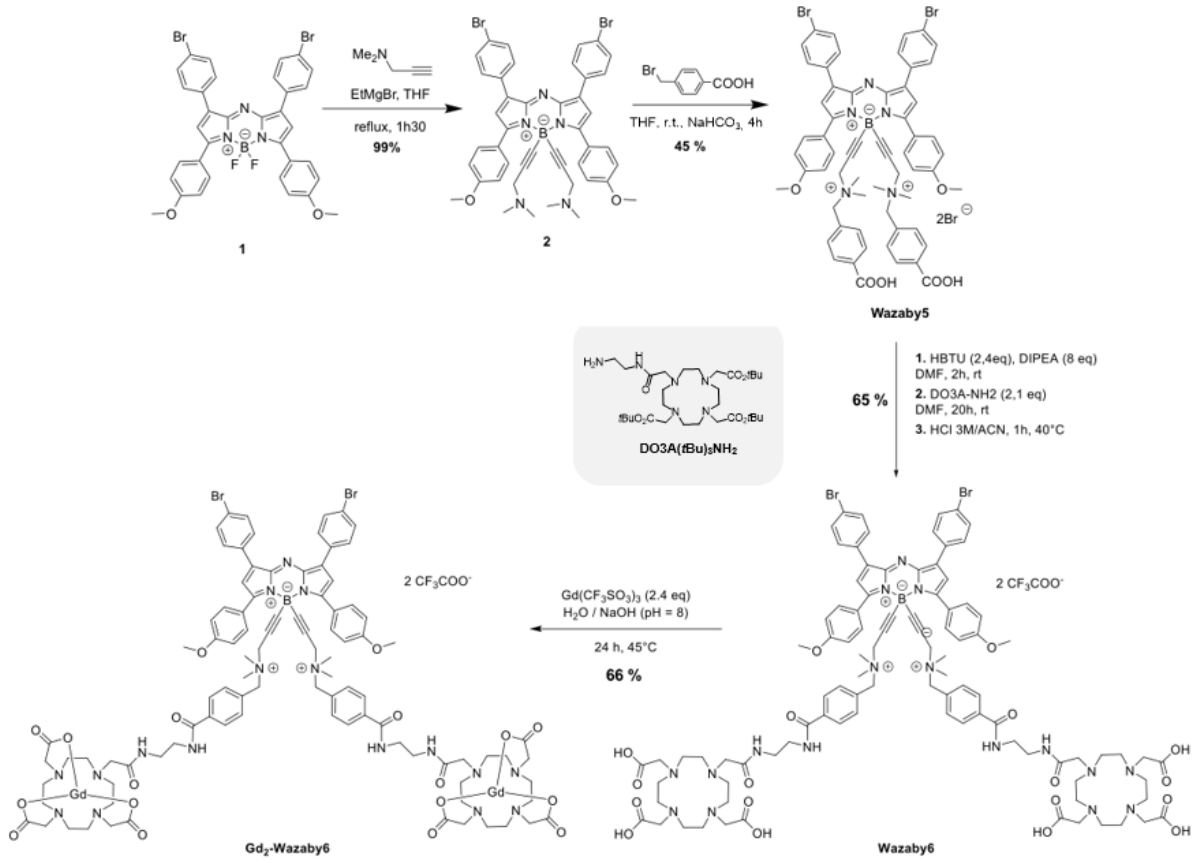

Scheme 1: synthetic route toward the bimodal probe ***Gd_2-Wazaby6***

Wazaby5 was reacted with a macrocyclic derivative (DO3A(*t*Bu)$_3$NH$_2$) in classic peptidic coupling reaction conditions and directly treated by HCl 3M in order to hydrolyze the protected tertiobutylester arms. The bis-DOTA derivative was then purified by semi-preparative HPLC to lead to the formation of pure **Wazaby6**. It is worth noting that the fluxionality of macrocycles implied to record NMR spectra at high temperature. A representation of variable temperature ^{1}H-NMR of **Wazaby6** is displayed in Figure S2.

Gadolinium was introduced into the two macrocycle cavities by reacting 2.4 eq of Gd(CF_3SO_3)$_3$ salt with **Wazaby6** in water in presence of sodium hydroxyde. The resulting homobimetallic complex **Gd_2-Wazaby6** was characterized by high resolution mass spectrometry (HRMS), HPLC, elemental analysis and ionic chromatography but not NMR due to its paramagnetic character.

Photophysical studies

As highlighted in the introduction, aza-BODIPY fluorophores display very interesting properties for *in vivo* optical imaging. However, in general, their main drawback is their poor solubility and their tendency to aggregate in water and in physiological media, despite the introduction of solubilizing groups. Most of the time, imaging experiments are performed in the presence of surfactants like Cremophor EL or castor oil.[39–42] Therefore, it was crucial for us to investigate the photophysical properties of our bimodal compounds in organic solvent (DMF, DMSO), as well as in PBS (Phosphate-Buffered Saline), without adding any surfactant.

*Table 1: photophysical data of **Wazaby5**, **Wazaby6**, and **Gd_2-Wazaby6** in different solvents at 298 K at 2 µM (λ_{exc} = 670 nm).*

Compound	Solvent	$\lambda_{max, Abs}$ [nm]	$\varepsilon_{\lambda max}$ [M^{-1} cm^{-1}]	$\lambda_{max, Em}$ [nm]	ϕ_F [%]*
Wazaby5	DMSO	704	74,000	739	29
Wazaby6	DMSO	705	82,000	741	15
	PBS	**705**	**46,000**	**741**	**10**
Gd_2-Wazaby6	DMSO	705	78,000	739	22
	PBS	**705**	**41,000**	**741**	**9**
	water	**705**	**49,000**	**741**	**10**

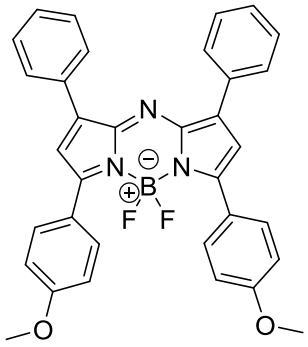

3

* reference: aza-BODIPY **3** (ϕ_F = 36% in chloroform, 298 K, λ_{exc} = 670 nm)[43]

The photophysical data of **Wazaby5**, **Wazaby6**, and the related bimetallic complex **Gd_2-Wazaby6** were studied in DMSO, DMF, and PBS, and results are depicted in Table 1, Figure 3, and Table S2. The three compounds display comparable absorption and emission profiles, with absorption wavelength at ≈705 nm and emission maxima at ≈740 nm. Interestingly, the introduction of the two macrocycles as well as the complexation of the two gadolinium atoms had almost no impact on the photophysical properties of the fluorophore.

When comparing **Wazaby6** and **Gd_2-Wazaby6** in DMSO and PBS, we can notice that the absorption, emission and excitation profiles of the compounds are comparable in both media (Figure 3), even if we can observe that absorption band is slightly larger than excitation one between 600 and 650 nm in PBS. It suggests that very limited aggregation occurs in PBS. If these spectra are compared to the ones of Kim's and Long's system,[28] it clearly highlights the interest of boron-functionalization for limiting aggregation phenomenon, which is really frequent for aza-BODIPY fluorophores. Interestingly, the quantum yield efficiency remains comparable both in organic solvents (around 20%) and in PBS (around 10%). Such values are good for NIR emitters and are clearly enough to undertake future OI experiments.

It is well known that the presence of "heavy atoms" induces an increase of the spin-orbit coupling and therefore promotes the generation of singlet oxygen.[32,44] However, this effect is generally more substantial when the heavy atoms occupy a position in the core region of the aza-BODIPY. In the present study, a non-toxic probe is under scope, thus, the production of singlet oxygen needs to be controlled. In order to test if toxic singlet oxygen is generated, the probes were dissolved in a non-protic solvent (DMF) for feasible observation of the phosphorescence band of singlet oxygen at 1270 nm, as protic solvents will efficiently quench its emission.[45] In every case this band was found to be absent, which confirms that neither **Wazaby6** nor **Gd_2-Wazaby6** produce singlet oxygen, when

irradiated (see supporting information for details). Moreover, preliminary antiproliferative tests on HepG2 cells (Human hepatocellular carcinoma, ATCC® HB-8065™) confirmed that **Gd_2-Wazaby6** do not display significant toxicity (IC_{50} at 24h > 100 µM). Additional experiments will be performed in the future to ascertain this aspect.

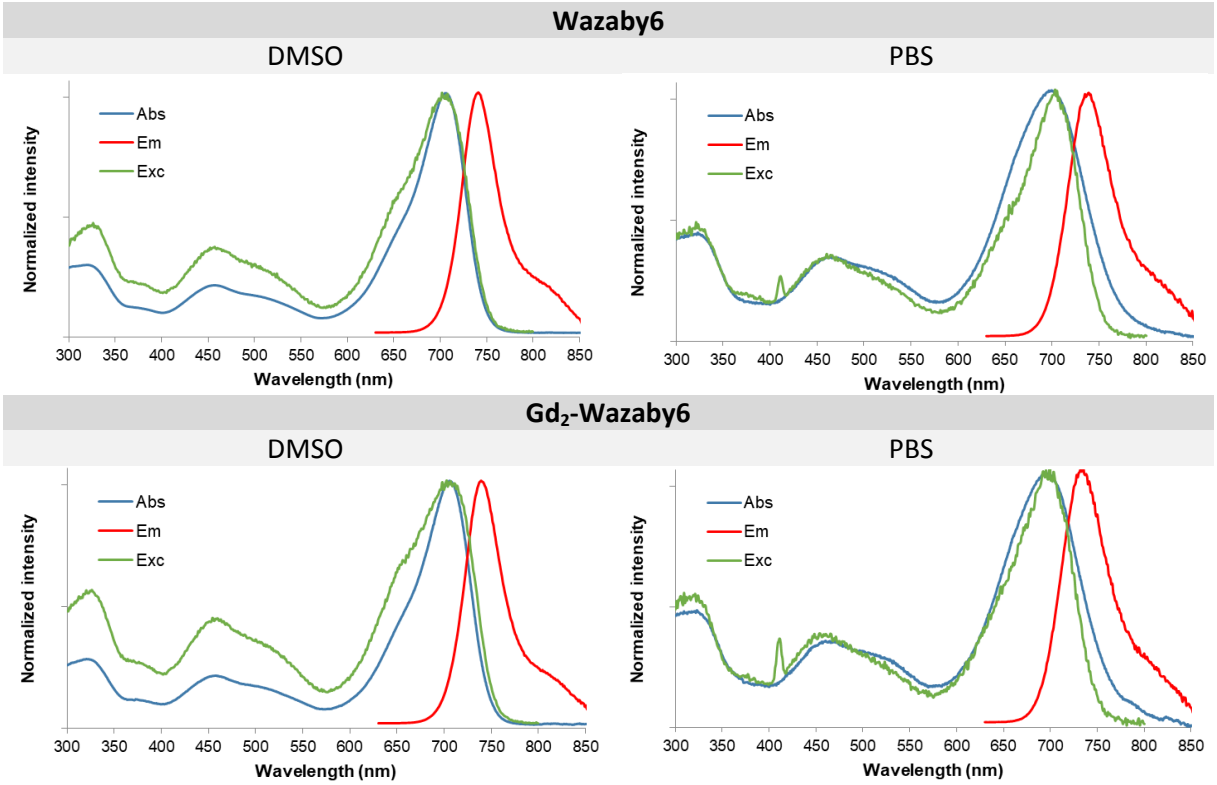

*Figure 3: Normalized absorption, emission, and excitation spectra of **Wazaby6** and **Gd_2-Wazaby6** at 298 K (λ_{ex} = 620 nm for emission spectra, detection at λ_{em} = 820 nm for excitation spectra)*

Relaxivity studies

Given the good solubility of the system, relaxivity measurements could be undertaken to characterize the efficiency of the system as an MRI probe. To this aim, NMRD (Nuclear Magnetic Resonance Dispersion) profiles were measured in water at 0.64 mM at pH = 7.2 in the field range 40 kHz – 400 MHz at two different temperatures (298 K and 310 K) as illustrated in Figure 4.

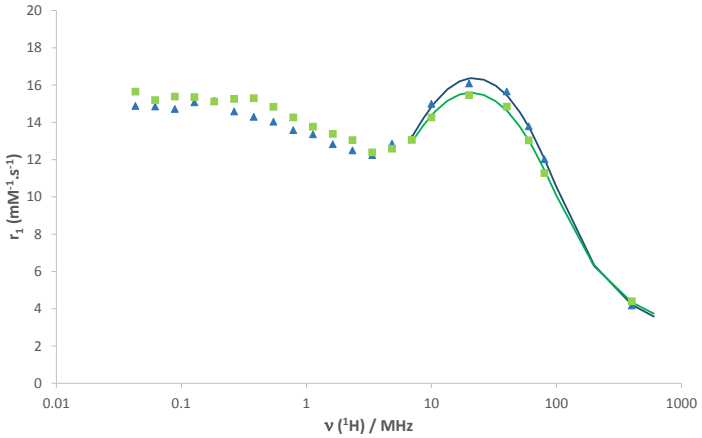

*Figure 4: ^{1}H NMRD profile of **Gd_2-Wazaby6** 0.64 mM in water, pH = 7.2 at 298 K (■) and 310 K (▲). The lines represent the best fit to the SBM theory.*

Interestingly, the temperature dependence of the system shows that we are in an intermediate regime where the rotation of the system starts to limit relaxivity rather than the water exchange rate. Indeed, the 37°C relaxivities are very close and even higher than those at 25°C. Typically, when the rotation is the limiting parameter (as observed for small molecular systems), relaxivity is decreasing when increasing temperature, whereas when the water exchange rate is limiting, relaxivity is increasing with increasing temperature. This result is also in accordance with the characteristic hump of slowly-rotating species visible on the NMRD profiles at intermediate fields (20-80 MHz). As this system remains quite flexible, we decided to investigate the relaxivity as a function of the Gd^{3+} concentration. Relaxivities were measured in the Gd^{3+} concentration range 0.1 – 4 mM (0.05 – 2 mM for the system) both in water at pH = 7.2 and in PBS at pH = 7.4, and the results are presented in Figure 5. At the concentration used for measuring relaxivities (0.64 mM of **Gd_2-Wazaby6**), we can see that some aggregation occurs both in water and PBS probably due to interactions between the aza-BODIPY units. This is in accordance with the photophysical studies, highlighting small aggregation, but which doesn't prevent water solubility. The aggregation is favored in PBS, which can be explained by additional electrostatic interactions between the **Gd_2-Wazaby6** cation (positive charge) and PBS (minus charge). This phenomenon certainly explains the temperature dependency of this otherwise quite flexible system.

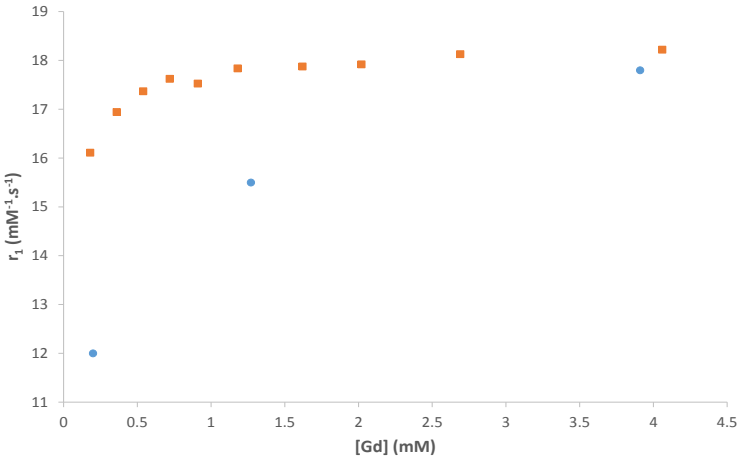

Figure 5: Relaxivity of the complex as a function of Gd^{3+} concentration at 298 K, 20 MHz, in water at pH = 7.2 (●) and in PBS at pH = 7.4 (■).

The relaxivity of the system at 0.64 mM in water and at 20 MHz, 310 K is 16.1 $mM^{-1}.s^{-1}$. As a comparison, and as expected due to the aggregation phenomenon, it is considerably higher than that of the mononuclear GdDOTA-BODIPY complex (3.9 $mM^{-1}.s^{-1}$)[13] and the relaxivity of the Bis-GdDTPA-aza-BODIPY system is 13.3 $mM^{-1}.s^{-1}$ at 60 MHz and room temperature[28] (see Figure S10 for structures). The relaxivity is in the same order of magnitude than a multimodal polyrotaxane comprising cyclodextrins bearing GdDOTAMA or BODIPYs (r_1 = 18.60 $mM^{-1}.s^{-1}$)[29] or a porphyrinic system DPP-ZnP-GdDOTA (see Figure S10; r_1 = 17.9 $mM^{-1}.s^{-1}$) presenting also some aggregation.[46] Finally, the relaxivity compares well with those of nanosized objects such as MOFs[47] and micelles[48,49].

In order to gain more insight into the parameters governing relaxivity, ^{17}O measurements as a function of temperature have been performed. Variable temperature ^{17}O T_2 measurements give access to the water exchange rate, k_{ex}. The ^{17}O T_1 data are determined by dipole-dipole and quadrupolar relaxation mechanisms and provide information about the rotational correlation time, τ_R. The ^{17}O chemical shifts give indication of the number of water molecules directly coordinated to Gd^{3+}, *q*. Longitudinal, transverse ^{17}O relaxation rates and chemical shifts were measured as a function of the temperature on aqueous solution of **Gd_2-Wazaby6** at 2.39 mM, and on a diamagnetic reference ($HClO_4$, pH 3.3) at 9.4 T. Due to the concentration used for the study, ^{17}O chemical shifts and T_1 values were too close to those of the reference to yield reliable data. Only ^{17}O T_2 data were analyzed and are presented in Figure 6.

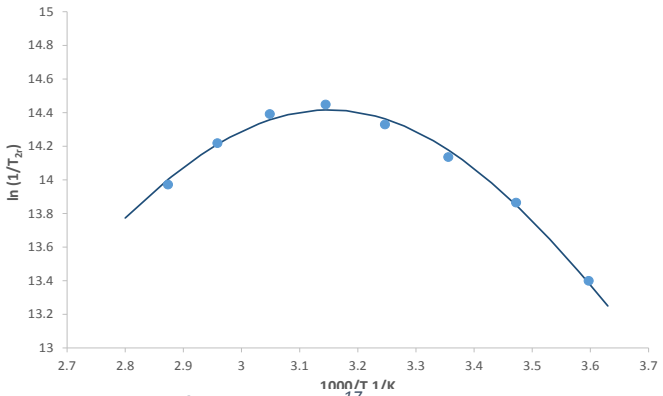

*Figure 6: Temperature dependence of the reduced ^{17}O transverse relaxation rates of **Gd_2-Wazaby6** (2.39 mM) at 9.4 T. The continuous curve represents the best fit to the experimental data points.*

The reduced ^{17}O transverse relaxation rates first increase (up to ca. 318 K), then decrease with increasing temperature indicating that the complex is in the slow kinetic region at low temperatures and in the fast exchange region at higher temperatures. In the slow kinetic region, $1/T_{2r}$ is directly determined by the exchange rate constant k_{ex}, whereas in the fast exchange region, it is determined by the transverse relaxation rate of the coordinated water oxygen, $1/T_{2m}$, which is in turn influenced by the water exchange rate, k_{ex}, the longitudinal electronic relaxation rate, $1/T_{1e}$, and the scalar coupling constant, $A/\hbar$.

Due to the different concentrations used for the ^{17}O NMR (4.78 mM of Gd^{3+}) and NMRD samples (1.27 mM of Gd^{3+}) and the aggregation process previously evidenced, the ^{17}O NMR and NMRD data have been analysed separately according to the Solomon-Bloembergen-Morgan theory.

Table 2 : Best-fit parameters obtained from the independent fitting of the ^{1}H NMRD profiles (Figure 4) to the SBM theory, including the Lipari-Szabo approach to describe internal flexibility and the transverse ^{17}O NMR relaxation rates as a function of temperature (Figure 6) at 9.4 T. The number in brackets represents the error on the last digit.

Parameters	**Gd_2-Wazaby6**	[DPP-ZnP-GdDOTA]$^{-}$ [c]	$GdDOTAC_{12}$ (micellar form)[d]	Zn-LZF2Gd[e]
r_1 ($mM^{-1}s^{-1}$; 20 MHz, 37°C)	16.1	17.9	17.9[b]	15.8
q[a]	1	1	1	1
k_{ex}^{298} (10^6 s^{-1})	2.81 [± 0.08]	4.1	4.9	1.6
$\Delta H^{\neq}$ ($kJ.mol^{-1}$)	40 [± 1]	49.8	52	40
$\Delta S^{\neq}$ ($J.K^{-1}.mol^{-1}$)	13 [± 3]	-	+ 67	-
E_l ($kJ.mol^{-1}$)	7 [± 4]	40	20	20
τ_l^{298} (ps)	111 [± 9]	245	430	145
E_g ($kJ.mol^{-1}$)	5 ± [1.5]	14	35	13
τ_g^{298} (ps)	1840 [± 70]	2640	1600	1160
S^2	0.30 [± 0.01]	0.26	0.23	0.64

[a] fixed in the fit; [b] at 60 MHz and 298 K; [c] From ref [46]; [d] From ref [48]; [e] From ref [50]

In the fitting procedure, the number of water molecules directly coordinated to Gd^{3+} was fixed to 1 as it is expected for GdDOTAMA complexes. In the fit of the proton relaxivities, the water exchange parameters were fixed to values obtained in the ^{17}O NMR study. The rotational dynamics could be only described by applying the Lipari-Szabo approach. In this approach, that separates local and global motions, characterized by the local and global rotational correlation times, τ_l^{298} and τ_g^{298}, respectively, and a model independent order parameter, S^2. It reflects the degree of spatial restriction of the local motion with respect to the global motion. Its value ranges from 0 to 1, with $S^2 = 0$ if the internal motions are isotropic, and $S^2 = 1$ if the internal motions are completely restricted.

The fitting has been restricted to frequencies above 6 MHz for NMRD data as at low magnetic fields the SBM theory fails in describing electronic parameters and rotational dynamics of slowly rotating species. Details of the analysis and the equations used in the fit are given in the Supporting Information, and the most important parameters obtained are listed in Table 2. A complete list of the parameters fitted for our system is also given Table S1.

For comparison, three other systems have been presented within the table (Table 2): a porphyrinic system with a GdDOTAGA appended (DPP-ZnP-GdDOTA); a $GdDOTAC_{12}$ complex in its micellar form, and a 30 aminoacid peptides derived from a Zn-finger peptide and bearing a GdDOTAMA complex in a folded form (Zn-bound form; Zn-LZF2Gd). They have been chosen because: (1) they have been all analyzed using the Lipari Szabo approach; (2) the porphyrinic system has a similar molecular weight as our system and shows some small aggregation as well; (3) the $GdDOTAC_{12}$ is in its micellar form which could "mimick" an aggregated state; (4) the peptidic system has a similar coordination sphere for Gd^{3+} than our system and the relaxivity behavior as a function of temperature is similar (relaxivity limited by rotation rather than water exchange rate).

The fitting of the ^{17}O data yields a value of k_{ex} of $2.81.10^6$ s^{-1}, which is lower than that of GdDOTA ($k_{ex} = 4.1.10^6$ s^{-1}) as expected when a carboxylate function is replaced by an amide function, and in the same range than other GdDOTAMA complexes (*ca.* 2.10^6 s^{-1}).[51] It suggests that the aggregation process, which certainly occurs through the BODIPY moiety, does not affect the water exchange rate of the system. The activation entropy calculated is also positive and in the same order of magnitude as that of complexes possessing similar coordination spheres. The water exchange mechanism has not been directly assessed (it is beyond the scope of this study), but the activation entropy calculated gives an indication of a dissociative mechanism as expected for nine-coordinated Gd^{3+} complexes. In dissociative mechanism, the steric crowding is of primary importance as the determining step is the dissociation of the water molecule. A highly-crowded environment will favour this dissociative activation step. As carboxylate functions are more coordinating than amide function, they imply more constraints explaining why GdDOTA complexes have higher water exchange rates than GdDOTAMA complexes.

The local and global correlation times of the system are within the same range as those of similar systems giving rise to similar relaxivities as shown in Table 2. The low value of S^2, comparable to those of DPP-ZnP-GdDOTA or the micellar system, shows that the motion of the Gd^{3+}-coordinated water proton vector is largely decoupled from the overall motion of the aggregates. This can be explained by the quite flexible chain between the Aza-BODIPY core and the Gd^{3+} complexes. If we look in more detail, the global correlation time of the system correlates well with that of the micellar system, or that of DPP-ZnP-GdDOTA having a similar molecular weight and presenting some aggregation. It is slightly higher than that of the peptidic system with a higher molecular weight but which is not in an aggregated form. All this confirms that some aggregation occurs for our system. The value of the local correlation time, consistent with that of a small Gd^{3+} complex, corroborates the flexibility around the Gd^{3+} complexes and shows that the aggregation certainly occurs through the aza-BODIPY core.

Finally, the temperature dependence of the relaxivity of our system is related to the low water exchange rate of the system together with a slow motion explained by the size of the complex and the presence of some aggregation. The same behavior is not observed with the porphyrinic system due to the difference in the water exchange rates (explained by the different Gd^{3+} coordination spheres). On the contrary, the peptidic system presents the same (even exacerbated) temperature behavior, which is explained by a more rigid system with slightly lower water exchange rate, despite the same Gd^{3+} coordination sphere. To sum up, the high relaxivity observed is due to the size of the system and the presence of some small aggregates.

Preliminary imaging studies on phantom and measurements in HSA

Phantom images of the system **Gd_2-Wazaby6** have been recorded both in MRI and in fluorescence to highlight its potential.

T_1-weighted images were recorded at 7 T, and show a greater contrast compared to the commercial GdDOTA at the same concentration (150 µM) (Figure 7).

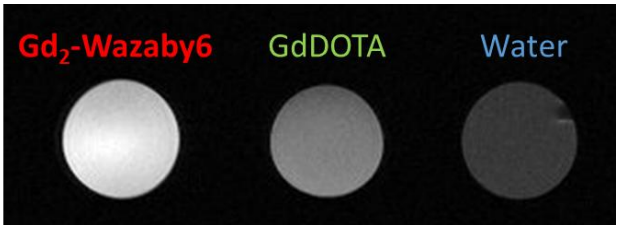

*Figure 7: T_1-weighted MRI phantom images of **Gd_2-Wazaby6** (150 µM), **GdDOTA** (150 µM) and water (reference) at 7 T using spin-echo sequence with TE = 50 ms and TR = 500 ms.*

Fluorescence images were recorded thanks to an optical imager for *in vivo* experiments (IVIS Lumina III, Perkin Elmer, *Figure 8*). **Gd_2-Wazaby6** was imaged at 150 µM (the concentration used for MRI imaging), 15 µM, and 1.5 µM in water; Aza-BODIPY **3** was imaged at 150 µM as a control. The first observation that can be made is the strong fluorescence of **Gd_2-Wazaby6** with respect to Aza-BODIPY **3** (**3** is not fluorescent due to its insolubility in water). Additionally, it is worth noting that **Gd_2-Wazaby6** displays higher fluorescence at 15 µM than at 150 µM, which corroborates the fact that some aggregation phenomenon can occur at high concentration. Moreover, we were pleased to note that a significant signal can be observed up to 850 nm, especially when exciting the molecule at 700 or 720 nm, meaning that **Gd_2-Wazaby6** can be detected wherever we want in biological window.

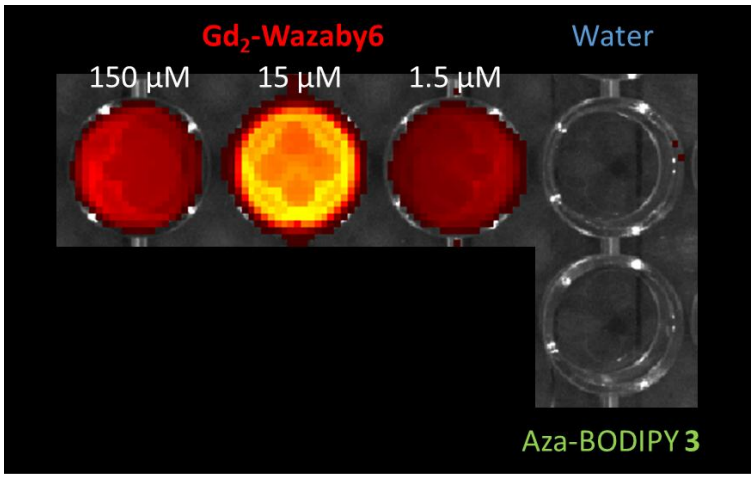

*Figure 8: Phantom optical images of of Gd_2-Wazaby6 (150 µM, 15 µM, and 1.5 µM), Aza-BODIPY **3** (150 µM), and water (reference) excitation at 660 nm and detection at 710 nm).*

The relaxivity and the optical emission properties of the system have also been measured in the presence of 0.6 mM of Human Serum Albumin (HSA) (physiological concentration) in order to simulate biological environment. Concerning the relaxivity of **Gd_2-Wazaby6** (at 145 µM), a 14 % increase is observed in water at pH = 7.3, 60 MHz, and 25°C, in the presence of HSA. This increase is explained by the formation of a supramolecular adduct between the probe and HSA as commonly observed for hydrophobic systems. Concerning the optical properties, the emission of **Gd2-Wazaby6** (at 2µM) increased by 230% in presence of HSA, probably due to the more lipophilic environment. The improved properties of **Gd2-Wazaby6** for both MRI and OI in presence of HSA are reassuring regarding its efficiency in real biological media.

These different preliminary studies are very promising for the future use of our probe for *in vivo* bimodal imaging.

Conclusion

For the first time, a monomolecular multimodal imaging probe for MRI and Near-Infrared Fluorescence (**Gd_2-Wazaby6**) was synthesized thanks to a boron functionalization of an aza-BODIPY. It was fully characterized by usual spectroscopic techniques. The boron functionalization allows good solubility of the system both in water and PBS and enables full photophysical and relaxometric characterizations. Interestingly, the quantum yield of fluorescence of this bimodal system is around 10% in PBS, which is particularly high for a near infrared fluorophore. Moreover, this probe does not induce the production of singlet oxygen, which could be toxic for biological tissue. The relaxivity observed for **Gd_2-Wazaby6** is high and can be explained both by the size of the system and the presence of some small aggregation process, as also observed in the optical imaging studies. Despite these aggregates the system remains very soluble in water and in biological media, and could be studied without the presence of surfactant as often needed with BODIPY derivatives. Those small aggregates do not imply important fluorescence quenching and enable to achieve high efficiency in MRI (in future work, it will be worth studying whether these small aggregates are still present *in vivo*). The relaxivity could also be further optimized by rigidifying the system and modifying the coordination sphere of Gd^{3+}, which is the subject of future studies. All together this suggests that these bimodal systems hold great promise as MRI and NIR probes *in vitro* and *in vivo* imaging.

Acknowledgments

The Ministère de l'Enseignement Supérieur et de la Recherche, the Centre National de la Recherche Scientifique (CNRS), the Conseil Régional de Bourgogne (PhD JCE grant # 2015-9205AAO033S04139 / BG0003203), and the French Research National Agency (ANR) via project JCJC ''SPID" ANR-16-CE07-0020 and project JCJC "WazaBY" ANR-18-CE18-0012 are gratefully acknowledged. This work is part of the projects ''Pharmacoimagerie et agents théranostiques" et ''Chimie durable, environnement et agroalimentaire" supported by the Université de Bourgogne and the Conseil Régional de Bourgogne through the Plan d'Actions Régional pour l'Innovation (PARI) and the European Union through the PO FEDER-FSE Bourgogne 2014/2020 programs. It was performed within the Dijon's pharmaco-imaging consortium, a regional center of excellence in pharmacoimaging. This work was also supported by a French Government Grant managed by the French National Research Agency (ANR) under the program "Investissements d'Avenir" (reference ANR-10-EQPX-05- 01/IMAPPI Equipex). Chematech® society is warmly thanked for providing DO3A-$(tBu)_3$-NH_2 macrocycle. FrenchBIC, GDR AIM, and OncoDesign® are acknowledged for fruitful discussion. LAG acknowledged the French Research National Agency (ANR) for her grant (SADAM ANR-16-CE07-0015-02). Mr Soustelle, and Ms M.-J. Penouilh are gratefully acknowledged for HR-MS, NMR analyses, and Dr Myriam Laly for ionic chromatography.

Supporting Information Available

This section gathered all experimental details: synthetic procedures, analytical data (^1H, ^{13}C, ^{11}B, ^{19}F NMR, HRMS), ^1H-NMR spectra, analytical and semi-preparative HPLC conditions and chromatograms, ionic chromatography, protocol for determining photophysical properties, absorption, emission and excitation spectra, photophysical experiments with or without HSA and on phantoms, structures of the systems discussed in the article, details concerning relaxometric measurements, temperature dependent ^{17}O measurements, relaxivity measurements in the presence of HAS, phantom MRI images, full parameters used in the fitting procedure of NMRD and ^{17}O data, and equations used for

the fits of ^{17}O NMR and ^{1}H NMRD data, report of singlet oxygen formation studies, and details of antiproliferative tests.

References

(1) Barabino, G.; Klein, J. P.; Porcheron, J.; Grichine, A.; Coll, J.-L.; Cottier, M. Intraoperative Near-Infrared Fluorescence Imaging Using Indocyanine Green in Colorectal Carcinomatosis Surgery: Proof of Concept. *Eur J Surg Oncol* **2016**, *42* (12), 1931–1937. https://doi.org/10.1016/j.ejso.2016.06.389.

(2) Frangioni, J. V. In Vivo Near-Infrared Fluorescence Imaging. *Curr Opin Chem Biol* **2003**, *7* (5), 626–634.

(3) Kiyose, K.; Aizawa, S.; Sasaki, E.; Kojima, H.; Hanaoka, K.; Terai, T.; Urano, Y.; Nagano, T. Molecular Design Strategies for Near-Infrared Ratiometric Fluorescent Probes Based on the Unique Spectral Properties of Aminocyanines. *Chemistry* **2009**, *15* (36), 9191–9200. https://doi.org/10.1002/chem.200900035.

(4) Yuan, L.; Lin, W.; Zheng, K.; He, L.; Huang, W. Far-Red to near Infrared Analyte-Responsive Fluorescent Probes Based on Organic Fluorophore Platforms for Fluorescence Imaging. *Chem Soc Rev* **2013**, *42* (2), 622–661. https://doi.org/10.1039/c2cs35313j.

(5) Zhu, H.; Fan, J.; Du, J.; Peng, X. Fluorescent Probes for Sensing and Imaging within Specific Cellular Organelles. *Acc. Chem. Res.* **2016**, *49* (10), 2115–2126. https://doi.org/10.1021/acs.accounts.6b00292.

(6) Guo, Z.; Park, S.; Yoon, J.; Shin, I. Recent Progress in the Development of Near-Infrared Fluorescent Probes for Bioimaging Applications. *Chem. Soc. Rev.* **2014**, *43* (1), 16–29. https://doi.org/10.1039/C3CS60271K.

(7) Zhao, J.; Chen, J.; Ma, S.; Liu, Q.; Huang, L.; Chen, X.; Lou, K.; Wang, W. Recent Developments in Multimodality Fluorescence Imaging Probes. *Acta Pharmaceutica Sinica B* **2018**, *8* (3), 320–338. https://doi.org/10.1016/j.apsb.2018.03.010.

(8) James, M. L.; Gambhir, S. S. A Molecular Imaging Primer: Modalities, Imaging Agents, and Applications. *Physiological Reviews* **2012**, *92* (2), 897–965. https://doi.org/10.1152/physrev.00049.2010.

(9) Hernot, S.; Manen, L. van; Debie, P.; Mieog, J. S. D.; Vahrmeijer, A. L. Latest Developments in Molecular Tracers for Fluorescence Image-Guided Cancer Surgery. *The Lancet Oncology* **2019**, *20* (7), e354–e367. https://doi.org/10.1016/S1470-2045(19)30317-1.

(10) Wang, Y.; Song, R.; Feng, H.; Guo, K.; Meng, Q.; Chi, H.; Zhang, R.; Zhang, Z. Visualization of Fluoride Ions In Vivo Using a Gadolinium(III)-Coumarin Complex-Based Fluorescence/MRI Dual-Modal Probe. *Sensors* **2016**, *16* (12), 2165. https://doi.org/10.3390/s16122165.

(11) Wang, Y.; Song, R.; Guo, K.; Meng, Q.; Zhang, R.; Kong, X.; Zhang, Z. A Gadolinium(III) Complex Based Dual-Modal Probe for MRI and Fluorescence Sensing of Fluoride Ions in Aqueous Medium and in Vivo. *Dalton Trans.* **2016**, *45* (44), 17616–17623. https://doi.org/10.1039/C6DT02229D.

(12) Harrison, V. S. R.; Carney, C. E.; MacRenaris, K. W.; Waters, E. A.; Meade, T. J. Multimeric Near IR–MR Contrast Agent for Multimodal In Vivo Imaging. *J. Am. Chem. Soc.* **2015**, *137* (28), 9108–9116. https://doi.org/10.1021/jacs.5b04509.

(13) Ceulemans, M.; Nuyts, K.; De Borggraeve, W.; Parac-Vogt, T. Gadolinium(III)-DOTA Complex Functionalized with BODIPY as a Potential Bimodal Contrast Agent for MRI and Optical Imaging. *Inorganics* **2015**, *3* (4), 516–533. https://doi.org/10.3390/inorganics3040516.

(14) Dong, D.; Jing, X.; Zhang, X.; Hu, X.; Wu, Y.; Duan, C. Gadolinium(III)–Fluorescein Complex as a Dual Modal Probe for MRI and Fluorescence Zinc Sensing. *Tetrahedron* **2012**, *68* (1), 306–310. https://doi.org/10.1016/j.tet.2011.10.034.
(15) Yamane, T.; Hanaoka, K.; Muramatsu, Y.; Tamura, K.; Adachi, Y.; Miyashita, Y.; Hirata, Y.; Nagano, T. Method for Enhancing Cell Penetration of Gd3+-Based MRI Contrast Agents by Conjugation with Hydrophobic Fluorescent Dyes. *Bioconjugate Chem.* **2011**, *22* (11), 2227–2236. https://doi.org/10.1021/bc200127t.
(16) You, Y.; Tomat, E.; Hwang, K.; Atanasijevic, T.; Nam, W.; Jasanoff, A. P.; Lippard, S. J. Manganese Displacement from Zinpyr-1 Allows Zinc Detection by Fluorescence Microscopy and Magnetic Resonance Imaging. *Chem. Commun.* **2010**, *46* (23), 4139–4141. https://doi.org/10.1039/C0CC00179A.
(17) Huynh, A. M.; Müller, A.; Kessler, S. M.; Henrikus, S.; Hoffmann, C.; Kiemer, A. K.; Bücker, A.; Jung, G. Small BODIPY Probes for Combined Dual ^{19} F MRI and Fluorescence Imaging. *ChemMedChem* **2016**, *11* (14), 1568–1575. https://doi.org/10.1002/cmdc.201600120.
(18) Stasiuk, G. J.; Minuzzi, F.; Sae-Heng, M.; Rivas, C.; Juretschke, H.-P.; Piemonti, L.; Allegrini, P. R.; Laurent, D.; Duckworth, A. R.; Beeby, A.; et al. Dual-Modal Magnetic Resonance/Fluorescent Zinc Probes for Pancreatic β-Cell Mass Imaging. *Chem. Eur. J.* **2015**, *21* (13), 5023–5033. https://doi.org/10.1002/chem.201406008.
(19) Wang, H.; Mu, X.; Yang, J.; Liang, Y.; Zhang, X.-D.; Ming, D. Brain Imaging with Near-Infrared Fluorophores. *Coordination Chemistry Reviews* **2019**, *380*, 550–571. https://doi.org/10.1016/j.ccr.2018.11.003.
(20) Hong, G.; Antaris, A. L.; Dai, H. Near-Infrared Fluorophores for Biomedical Imaging. *Nat Biomed Eng* **2017**, *1* (1), 0010. https://doi.org/10.1038/s41551-016-0010.
(21) Hilderbrand, S. A.; Weissleder, R. Near-Infrared Fluorescence: Application to in Vivo Molecular Imaging. *Current Opinion in Chemical Biology* **2010**, *14* (1), 71–79. https://doi.org/10.1016/j.cbpa.2009.09.029.
(22) Li, J.-B.; Liu, H.-W.; Fu, T.; Wang, R.; Zhang, X.-B.; Tan, W. Recent Progress in Small-Molecule Near-IR Probes for Bioimaging. *Trends in Chemistry* **2019**, *1* (2), 224–234. https://doi.org/10.1016/j.trechm.2019.03.002.
(23) Martinić, I.; Eliseeva, S. V.; Petoud, S. Near-Infrared Emitting Probes for Biological Imaging: Organic Fluorophores, Quantum Dots, Fluorescent Proteins, Lanthanide(III) Complexes and Nanomaterials. *Journal of Luminescence* **2017**, *189*, 19–43. https://doi.org/10.1016/j.jlumin.2016.09.058.
(24) Haque, A.; Faizi, Md. S. H.; Rather, J. A.; Khan, M. S. Next Generation NIR Fluorophores for Tumor Imaging and Fluorescence-Guided Surgery: A Review. *Bioorganic & Medicinal Chemistry* **2017**, *25* (7), 2017–2034. https://doi.org/10.1016/j.bmc.2017.02.061.
(25) Garland, M.; Yim, J. J.; Bogyo, M. A Bright Future for Precision Medicine: Advances in Fluorescent Chemical Probe Design and Their Clinical Application. *Cell Chemical Biology* **2016**, *23* (1), 122–136. https://doi.org/10.1016/j.chembiol.2015.12.003.
(26) Ge, Y.; O'Shea, D. F. Azadipyrromethenes: From Traditional Dye Chemistry to Leading Edge Applications. *Chem. Soc. Rev.* **2016**, *45* (14), 3846–3864. https://doi.org/10.1039/C6CS00200E.
(27) Pliquett, J.; Dubois, A.; Racoeur, C.; Mabrouk, N.; Amor, S.; Lescure, R.; Bettaïeb, A.; Collin, B.; Bernhard, C.; Denat, F.; et al. A Promising Family of Fluorescent Water-Soluble Aza-BODIPY Dyes for in Vivo Molecular Imaging. *Bioconjugate Chem.* **2019**, *30* (4), 1061–1066. https://doi.org/10.1021/acs.bioconjchem.8b00795.
(28) Kim, E.-J.; Bhuniya, S.; Lee, H.; Kim, H. M.; Shin, W. S.; Kim, J. S.; Hong, K. S. In Vivo Tracking of Phagocytic Immune Cells Using a Dual Imaging Probe with

Gadolinium-Enhanced MRI and Near-Infrared Fluorescence. *ACS Appl. Mater. Interfaces* **2016**, *8* (16), 10266–10273. https://doi.org/10.1021/acsami.6b03344.
(29) Fredy, J. W.; Scelle, J.; Guenet, A.; Morel, E.; Adam de Beaumais, S.; Ménand, M.; Marvaud, V.; Bonnet, C. S.; Tóth, E.; Sollogoub, M.; et al. Cyclodextrin Polyrotaxanes as a Highly Modular Platform for the Development of Imaging Agents. *Chemistry – A European Journal* **2014**, *20* (35), 10915–10920. https://doi.org/10.1002/chem.201403635.
(30) Wu, D.; Daly, H. C.; Conroy, E.; Li, B.; Gallagher, W. M.; Cahill, R. A.; O'Shea, D. F. PEGylated BF2-Azadipyrromethene (NIR-AZA) Fluorophores, for Intraoperative Imaging. *European Journal of Medicinal Chemistry* **2019**, *161*, 343–353. https://doi.org/10.1016/j.ejmech.2018.10.046.
(31) Yang, Z.; Bai, X.; Ma, S.; Liu, X.; Zhao, S.; Yang, Z. A Benzoxazole Functionalized Fluorescent Probe for Selective Fe^{3+} Detection and Intracellular Imaging in Living Cells. *Anal. Methods* **2017**, *9* (1), 18–22. https://doi.org/10.1039/C6AY02660E.
(32) Bodio, E.; Denat, F.; Goze, C. BODIPYS and Aza-BODIPYS Derivatives as Promising Fluorophores for in Vivo Molecular Imaging and Theranostic Applications. *J. Porphyrins Phthalocyanines* **2019**, S1088424619501268. https://doi.org/10.1142/S1088424619501268.
(33) Daly, H. C.; Sampedro, G.; Bon, C.; Wu, D.; Ismail, G.; Cahill, R. A.; O'Shea, D. F. BF 2 -Azadipyrromethene NIR-Emissive Fluorophores with Research and Clinical Potential. *European Journal of Medicinal Chemistry* **2017**, *135*, 392–400. https://doi.org/10.1016/j.ejmech.2017.04.051.
(34) Grossi, M.; Morgunova, M.; Cheung, S.; Scholz, D.; Conroy, E.; Terrile, M.; Panarella, A.; Simpson, J. C.; Gallagher, W. M.; O'Shea, D. F. Lysosome Triggered Near-Infrared Fluorescence Imaging of Cellular Trafficking Processes in Real Time. *Nat Commun* **2016**, *7* (1), 10855. https://doi.org/10.1038/ncomms10855.
(35) Bellier, Q.; Pégaz, S.; Aronica, C.; Le Guennic, B.; Andraud, C.; Maury, O. Near-Infrared Nitrofluorene Substitued Aza-Boron-Dipyrromethenes Dyes. *Org. Lett.* **2011**, *13* (1), 22–25. https://doi.org/10.1021/ol102701v.
(36) Brücher, E.; Tircsó, G.; Baranyai, Z.; Kovács, Z.; Sherry, A. D. Stability and Toxicity of Contrast Agents. In *The Chemistry of Contrast Agents in Medical Magnetic Resonance Imaging*; John Wiley & Sons, Ltd, 2013; pp 157–208. https://doi.org/10.1002/9781118503652.ch4.
(37) Wahsner, J.; Gale, E. M.; Rodríguez-Rodríguez, A.; Caravan, P. Chemistry of MRI Contrast Agents: Current Challenges and New Frontiers. *Chem. Rev.* **2019**, *119* (2), 957–1057. https://doi.org/10.1021/acs.chemrev.8b00363.
(38) Loudet, A.; Bandichhor, R.; Wu, L.; Burgess, K. Functionalized BF2 Chelated Azadipyrromethene Dyes. *Tetrahedron* **2008**, *64* (17), 3642–3654. https://doi.org/10.1016/j.tet.2008.01.117.
(39) Jing, X.; Yu, F.; Chen, L. Visualization of Nitroxyl (HNO) in Vivo via a Lysosome-Targetable near-Infrared Fluorescent Probe. *Chem. Commun.* **2014**, *50* (91), 14253–14256. https://doi.org/10.1039/C4CC07561G.
(40) Bhuniya, S.; Lee, M. H.; Jeon, H. M.; Han, J. H.; Lee, J. H.; Park, N.; Maiti, S.; Kang, C.; Kim, J. S. A Fluorescence off–on Reporter for Real Time Monitoring of Gemcitabine Delivery to the Cancer Cells. *Chem. Commun.* **2013**, *49* (64), 7141–7143. https://doi.org/10.1039/C3CC42653J.
(41) Kamkaew, A.; Burgess, K. Aza-BODIPY Dyes with Enhanced Hydrophilicity. *Chem. Commun.* **2015**, *51* (53), 10664–10667. https://doi.org/10.1039/C5CC03649F.
(42) Daly, H. C.; Sampedro, G.; Bon, C.; Wu, D.; Ismail, G.; Cahill, R. A.; O'Shea, D. F. BF2-Azadipyrromethene NIR-Emissive Fluorophores with Research and Clinical

Potential. *Eur J Med Chem* **2017**, *135*, 392–400. https://doi.org/10.1016/j.ejmech.2017.04.051.
(43) Brouwer, A. M. Standards for Photoluminescence Quantum Yield Measurements in Solution (IUPAC Technical Report). *Pure and Applied Chemistry* **2011**, *83* (12), 2213–2228. https://doi.org/10.1351/PAC-REP-10-09-31.
(44) Karatay, A.; Miser, M. C.; Cui, X.; Küçüköz, B.; Yılmaz, H.; Sevinç, G.; Akhüseyin, E.; Wu, X.; Hayvali, M.; Yaglioglu, H. G.; et al. The Effect of Heavy Atom to Two Photon Absorption Properties and Intersystem Crossing Mechanism in Aza-Boron-Dipyrromethene Compounds. *Dyes and Pigments* **2015**, *122*, 286–294. https://doi.org/10.1016/j.dyepig.2015.07.002.
(45) *Singlet Oxygen*; 2016; Vol. 1. https://doi.org/10.1039/9781782622208.
(46) Schmitt, J.; Heitz, V.; Sour, A.; Bolze, F.; Kessler, P.; Flamigni, L.; Ventura, B.; Bonnet, C. S.; Tóth, É. A Theranostic Agent Combining a Two-Photon-Absorbing Photosensitizer for Photodynamic Therapy and a Gadolinium(III) Complex for MRI Detection. *Chemistry – A European Journal* **2016**, *22* (8), 2775–2786. https://doi.org/10.1002/chem.201503433.
(47) Carné-Sánchez, A.; Bonnet, C. S.; Imaz, I.; Lorenzo, J.; Tóth, É.; Maspoch, D. Relaxometry Studies of a Highly Stable Nanoscale Metal–Organic Framework Made of Cu(II), Gd(III), and the Macrocyclic DOTP. *J. Am. Chem. Soc.* **2013**, *135* (47), 17711–17714. https://doi.org/10.1021/ja4094378.
(48) Nicolle, G. M.; Tóth, É.; Eisenwiener, K.-P.; Mäcke, H. R.; Merbach, A. E. From Monomers to Micelles: Investigation of the Parameters Influencing Proton Relaxivity. *J Biol Inorg Chem* **2002**, *7* (7), 757–769. https://doi.org/10.1007/s00775-002-0353-3.
(49) Martins, A. F.; Morfin, J.-F.; Geraldes, C. F. G. C.; Tóth, É. Gd3+ Complexes Conjugated to Pittsburgh Compound B: Potential MRI Markers of β-Amyloid Plaques. *J Biol Inorg Chem* **2014**, *19* (2), 281–295. https://doi.org/10.1007/s00775-013-1055-8.
(50) Isaac, M.; Pallier, A.; Szeremeta, F.; Bayle, P.-A.; Barantin, L.; Bonnet, C. S.; Sénèque, O. MRI and Luminescence Detection of Zn2+ with a Lanthanide Complex–Zinc Finger Peptide Conjugate. *Chem. Commun.* **2018**, *54* (53), 7350–7353. https://doi.org/10.1039/C8CC04366C.
(51) *The Chemistry of Contrast Agents in Medical Magnetic Resonance Imaging: Helm/The Chemistry of Contrast Agents in Medical Magnetic Resonance Imaging*; Merbach, A., Helm, L., Tóth, É., Eds.; John Wiley & Sons, Ltd: Chichester, UK, 2013; Vol. Ch.2, p.25. https://doi.org/10.1002/9781118503652.
(52) Raiford, D. S.; Fisk, C. L.; Becker, E. D. Calibration of Methanol and Ethylene Glycol Nuclear Magnetic Resonance Thermometers. *Anal. Chem.* **1979**, *51* (12), 2050–2051. https://doi.org/10.1021/ac50048a040.
(53) Meiboom, S.; Gill, D. Modified Spin- Echo Method for Measuring Nuclear Relaxation Times. *Review of Scientific Instruments* **1958**, *29* (8), 688–691. https://doi.org/10.1063/1.1716296.
(54) Micskei, K.; Helm, L.; Brucher, E.; Merbach, A. E. Oxygen-17 NMR Study of Water Exchange on Gadolinium Polyaminopolyacetates [Gd(DTPA)(H2O)]2- and [Gd(DOTA)(H2O)]- Related to NMR Imaging. *Inorg. Chem.* **1993**, *32* (18), 3844–3850. https://doi.org/10.1021/ic00070a013.
(55) Hugi, A. D.; Helm, L.; Merbach, A. E. Water Exchange on Hexaaquavanadium(III): a Variable-Temperature and Variable-Pressure17O-NMR Study at 1.4 and 4.7 Tesla. *Helv. Chim. Acta* **1985**, *68* (2), 508–521. https://doi.org/10.1002/hlca.19850680224.

TOC Graphic

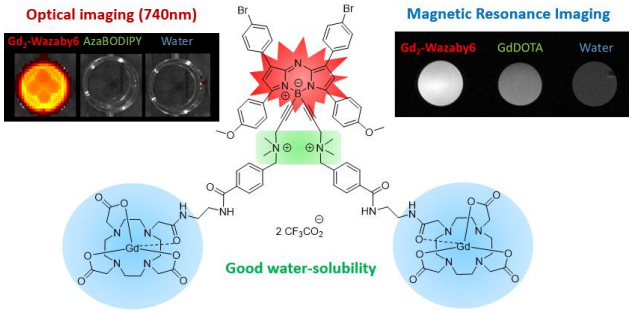

Synthesis and characterization of an original aza-BODIPY system comprising two Gd^{3+} complexes for magnetic resonance imaging (MRI)/optical imaging (OI) application, by functionalization of the boron center. This is the first aza-BODIPY based bimodal probe displaying a high brightness in near infrared fluorescence (λ_{em} = 740 nm), an excellent relaxivity for MRI, and displaying good water solubility. The novel bimodal probe possesses all the requirements for *in vivo* application.